

Phase-field study of grain boundary tracking behavior in crack-seal microstructures

Kumar Ankit^{a,*}, Britta Nestler^a, Michael Selzer^a, Mathias Reichardt^a

^aKarlsruhe Institute of Technology (KIT), IAM-ZBS, Haid-und-Neu-Str. 7, D-76131 Karlsruhe, Germany

Abstract

In order to address the vein-growth problem in geology, a multi-phase-field model is used to capture the dynamics of crystals precipitating from a super-saturated solution. To gain a detailed understanding, we investigate the influence of various boundary conditions on crystal growth. In particular, we analyze the formation of vein microstructures resulting from the free growth of crystals as well as crack-sealing processes. To define the crystal symmetry, we consider the anisotropy in surface energy to simulate crystals with flat facets and sharp corners, possessing different orientations and study the resulting growth competition to deduce a consistent orientation selection rule in the free-growth regime. From crack-sealing simulations, we correlate the grain boundary tracking behavior depending on the relative rate of crack opening, the performed trajectory, initial grain size and wall roughness. Further, we illustrate how these parameters induce the microstructural transition between blocky (crystals growing anisotropically) to fibrous morphology (isotropic) and formation of grain boundaries. The phase-field simulations of crystals in free-growth regime (in 2D and 3D) indicate that the growth or consumption of a crystal is dependent on the orientation difference with neighboring crystals. The crack-sealing simulation results (in 2D and 3D) reveal that crystals grow isotropically and grain boundaries track the opening trajectory if the wall roughness is high, opening increments are small and crystals touch the wall before the next crack increment starts. Further, we find that within the complete crack-seal regime, anisotropy in surface energy results in the formation of curved/oscillating grain boundaries (instead of straight) when the crack opening velocity is increased and wall roughness is not sufficiently high.

Keywords: Phase-field method, Crystal growth, Anisotropic surface energy, Veins

*Corresponding author. Tel.: +49 721 608-45022.

Email address: kumar.ankit@hs-karlsruhe.de (Kumar Ankit)

1. Introduction

Veins are sub-planar discontinuities in the earth's crust, containing minerals which precipitate from a super-saturated solution in a fracture (Urai et al., 1991). The microstructures from veins provide information on how fluids migrate through the crust, and how material is transferred by these fluids (Barker et al., 2006; Cox et al., 1987; Jamtveit and Yardley, 1997). They exhibit a wide range of crystal habits from dendritic, acicular to crystalline or fibrous structures depending on the boundary conditions (Bons and Jessell, 1997; Fisher and Brantley, 1992; Ramsay and Huber, 1983). Examples of such boundary conditions are: relative time of crystal growth with respect to fracture opening, degree of crack surface roughness, fluid properties (pressure, temperature, flow velocity and supersaturation) (Cox et al., 1987; Knipe and McCaig, 1994) or transport mechanisms (diffusion and advection) (Durney, 1976; McCaig, 1988; Yardley and Jamtveit, 1997). The morphology of crystals growing in freely flowing fluid differs significantly from the crystals growing in a constrained environment such as present in crack-sealing conditions. Among the numerous distinguishable crystal morphologies that develop due to a combination of boundary conditions, an interesting case is the formation of curved crystals in veins. Taber (1918) and Mügge (1928) explain a mechanism by which the crystal growth competition is suppressed owing to the presence of an external boundary condition. The authors discuss tracking of grain boundaries following the prescribed crack opening trajectory. Williams and Urai (1989) elucidate that the primary reason responsible for such deviations from the equilibrium crystal shape is mechanical coupling of wall rock and evolving crystals. Further, Hilgers and Urai (2002b) amend that mechanical coupling of vein and wall is not a necessary condition for the formation of curved fibrous crystals, if the crack increments are smaller than about 10 μm .

Durney and Ramsay (1973) propose that the syntectonic fibres grow along the opening trajectory with the transport mechanism being diffusion into the dilational sites. The process is assumed to be continuous, neglecting both the formation of significant fluid-filled openings as well as kinematic aspects. As an alternative to diffusional and continuous accretion, Ramsay (1980) discusses the discontinuous crack-seal mechanism, a repeated process of crack opening and sealing, as indicated by the characteristic inclusion bands/trails and stair-stepped grain boundaries. In recent papers based on experiments and theoretical modeling (Bons and Jessell, 1997; Fisher and Brantley, 1992), it is suggested that fibers can only form by a diffusional accretion process.

Cox and Etheridge (1983) and Urai et al. (1991) propose a kinematic model for crystal growth in crack seal veins and show the importance of the wall-rock morphology for the resulting vein microstructure. According to this model, if the crystals have already sealed the space available before the next crack event, the facets are lost and they assume the morphology of the rough vein wall interface. If opening increments are sufficiently small, the crystals cannot develop crystal facets and therefore, grow isotropically. An important conclusion of this model is that the crystal growth kinetics is effectively isotropic if the crack surface is sufficiently rough and crack opening rate is small. As a step to implement crystal anisotropy in 2D, an efficient numerical program *Vein Growth* is developed by Bons (2001) which is further utilized to simulate the anisotropic growth of crystals under complex boundary conditions. Simulations with *Vein Growth* produce fibrous crystals with the potential to track the opening trajectory of the crack when the wall morphology is rough and the average opening velocity is smaller than the growth velocity of the crystals (Hilgers et al., 2001; Koehn et al., 2000). A 2D simulation program FACET is separately developed by Zhang and Adams (2002) to study the growth of polycrystals based on deposition flux of atoms. Nollet et al. (2006) use the algorithms *Vein Growth* and FACET to study crystal growth competition leading to orientation selection and transition from blocky to fibrous morphology during crack-seal growth.

The numerical programs *Vein Growth* and FACET suffer from geometric restrictions and are vulnerable to inaccuracies at triple/quadruple crystal junctions. The artifacts of the algorithm *Vein Growth* namely ‘Crystal terminations’ and ‘Long-distance effects’ cause the euhedral angles between facets at crystal terminations to depart from angle corresponding to equilibrium shape and effect of non-neighbouring crystals is observed on growth process respectively. Further, the method advocates the switching of the numerical program to FACET in order to produce *crystallographically correct* facets that develop during free growth of crystals. However, the switching of numerical program induces new complication; the complete sealing of crack can no longer be simulated correctly. Besides, the algorithm FACET is not capable of generating the crystal facets from a randomly shaped nucleus and implicitly assumes the presence of *crystallographically correct* facets prior to growth process. We recognise that since neither of the methods used in the past are able to completely describe the crystal growth in veins and a three-dimensional microstructure formation, it is important to develop better algorithms to enhance the knowledge concerning the vein growth process.

The phase-field method, which is a well known diffuse interface method can overcome many of the problems suffered by earlier models such as the *Vein Growth* and FACET. It is an elegant and versatile way to tackle complicated moving boundary problems where interfacial energy plays an important role, without explicitly tracking the interface. The

model equations are derived on the basis of general thermodynamic and kinetic principles and contain a number of phenomenological parameters related to the physical properties of the material. These parameters are determined based on experimental and theoretical information. Different thermodynamic driving forces for microstructure evolution, such as chemical bulk free energy, interfacial energy, elastic strain energy and different transport processes, such as mass diffusion and advection, can be coupled and the effect on the over all evolution process can be studied simultaneously.

In the following article, we use a thermodynamically consistent multi-phase-field model (Nestler et al., 2005; Stinner et al., 2004) to resolve the ambiguity regarding the vein-growth mechanism. The structure of the article is organized as follows: in section 2, we present the specific formulation of the phase-field model for polycrystal growth by considering anisotropy of the surface energy to produce flat facets and sharp corners (Nestler et al., 2005; Stinner et al., 2004). In section 3 we analyze the kinematic properties of the anisotropic growth competition of crystals arising due to orientation difference with respect to the neighboring crystals. In section 4, we study the crystal growth process in crack-sealing conditions. The following sub-sections 4.1, 4.2, 4.3 and 4.4 deal with the influence of crack surface roughness, crack opening velocity, opening trajectory and number of crystal nuclei on the vein microstructure respectively. A detailed discussion of the 2D and 3D phase-field simulation results is presented in Section 5. Section 6 concludes the article with a view of future work that should be done to extend the present vein-growth model.

2. Phase-field model

We consider a set of phase-field parameters, denoted by $\phi(\vec{x}, t) = (\phi_1(\vec{x}, t) \cdots \phi_N(\vec{x}, t))$ where each component of the vector $\phi_\alpha(\vec{x}, t)$ varies smoothly from 1 inside 0 outside the crystal α over a small finite distance ε (diffuse interface). The location of the crystal-liquid or crystal-crystal interface is defined by a level set at $\phi_\alpha(\vec{x}, t) = 0.5$ which is determined mathematically by solving the evolution equation. The external fields like temperature or concentration can be coupled to the phase-field parameter ϕ , hence no external boundary conditions needs to be applied at the interfaces.

In this article, we use the phase-field equations derived from non-equilibrium thermodynamics guaranteeing a locally positive entropy production. The model is well suited to describe a polycrystalline system by accounting for an arbitrary number of phase-field parameters (Nestler et al., 2005). In the considered applications to crystal growth in veins, we restrict model definition to an isothermal problem. The Helmholtz free energy functional can be formulated as

$$\mathcal{F}(\phi) = \int_{\Omega} \left(f(\phi) + \varepsilon a(\phi, \nabla \phi) + \frac{1}{\varepsilon} w(\phi) \right) dx, \quad (1)$$

where $f(\phi)$ is the bulk free energy density, ε is the small length scale parameter related to the interface width, $a(\phi, \nabla \phi)$ is a gradient type and $w(\phi)$, a potential type energy density. We discuss each of these terms in detail.

The phase-field parameter $\phi(\vec{x}, t) = (\phi_1(\vec{x}, t) \cdots \phi_N(\vec{x}, t))$ describes the location of ‘N’ crystals with different orientation. The value of each phase field parameter ϕ_α lies in the interval $[0, 1]$ and fulfils the constraint $\sum_{\alpha=1}^N \phi_\alpha = 1$. The integral shown in functional (1) extends over the entire domain of consideration.

The gradient energy density $a(\phi, \nabla \phi)$ is given by

$$a(\phi, \nabla \phi) = \sum_{\substack{\alpha, \beta=1 \\ (\alpha < \beta)}}^{N, N} \gamma_{\alpha\beta} a_{\alpha\beta}^2(\phi, \nabla \phi) |\vec{q}_{\alpha\beta}|^2 \quad (2)$$

where $a_{\alpha\beta}(\phi, \nabla \phi)$ defines the form of the surface energy anisotropy of the evolving phase boundary and $\gamma_{\alpha\beta}$ is the surface free energy per unit area of the $\alpha - \beta$ boundary which may additionally depend on the relative orientation of the interface. The vector quantity $\vec{q}_{\alpha\beta} = \phi_\alpha \nabla \phi_\beta - \phi_\beta \nabla \phi_\alpha$ is a generalized gradient vector normal to the $\alpha - \beta$ interface. To assign an isotropic surface energy to the $\alpha - \beta$ phase boundary, $a_{\alpha\beta} = 1$ is chosen. For including a strongly anisotropic surface energy, so that crystals develop flat facets and sharp corners according to directions of the crystal symmetry, a piecewise defined function is used

$$a_{\alpha\beta}(\phi, \nabla \phi) = \max_{1 \leq k \leq \eta_{\alpha\beta}} \left\{ \frac{\vec{q}_{\alpha\beta}}{|\vec{q}_{\alpha\beta}|} \cdot \vec{\eta}_{\alpha\beta} \right\} \quad (3)$$

where $\{\vec{\eta}_{k, \alpha\beta} | k = 1, \dots, \eta_{\alpha\beta}\}$ for $\eta_{\alpha\beta} \in M$ denotes the complete set of vertex vectors of the corresponding Wulff shape of a crystal α embedded in the bulk phase β and M represents the number of edges. In figs. 1a and 1b, a polar plot of function (3) for a cubic symmetry and for a truncated octahedral shape are shown. The corresponding equilibrium crystal shapes are displayed in figs. 1c and 1d, respectively.

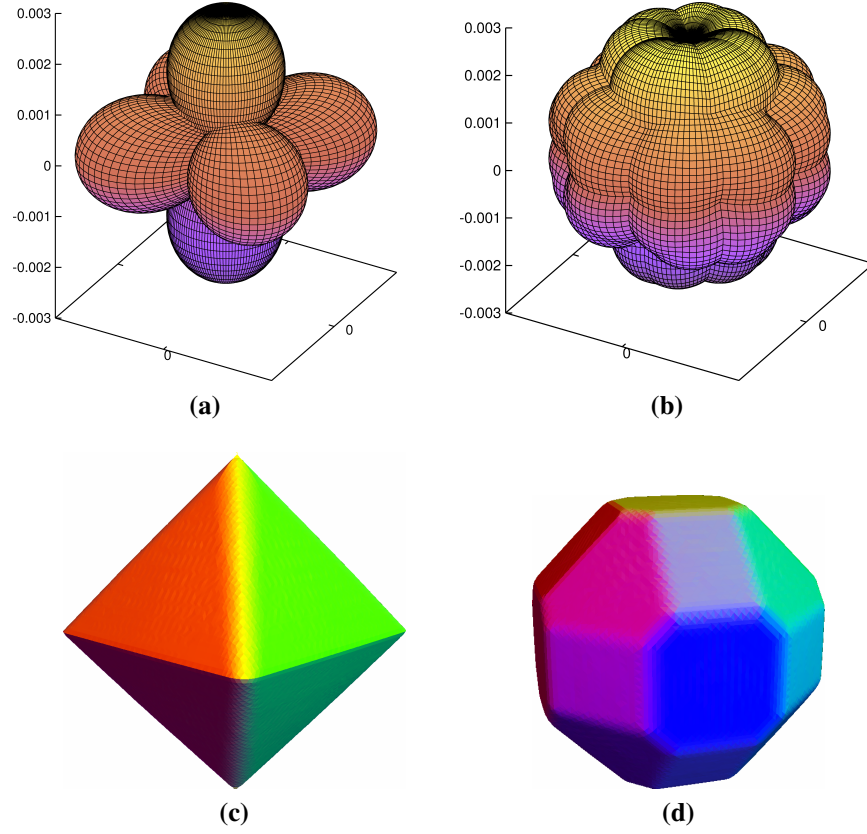


Figure 1: Polar plot of function (3) for (a) cubic and (b) alum (truncated octahedral symmetry). These anisotropic functions are incorporated in phase-field model to simulate the equilibrium crystal shapes for (c) an octahedral crystal and (d) an alum in free growth conditions. The colors in figs. 1c and 1d differentiate among crystal facets.

In the free energy functional (1), we choose the function $w(\phi)$ to represent a multi-obstacle potential in the form of

$$w(\phi) = \begin{cases} \frac{16}{\pi^2} \sum_{\substack{\alpha, \beta=1 \\ (\alpha < \beta)}}^{N,N} \gamma_{\alpha\beta} \phi_\alpha \phi_\beta + \sum_{\substack{\alpha, \beta, \delta=1 \\ (\alpha < \beta < \delta)}}^{N,N,N} \gamma_{\alpha\beta\delta} \phi_\alpha \phi_\beta \phi_\delta & \text{if } \phi \in \Sigma \\ \infty & \text{elsewhere} \end{cases} \quad (4)$$

where $\Sigma = \left\{ \phi \mid \sum_{\alpha=1}^N \phi_\alpha = 1 \text{ and } \phi_\alpha \geq 0 \right\}$. The higher order term proportional to $\phi_\alpha \phi_\beta \phi_\delta$ in function (4) is added to reduce the presence of unwanted third or higher-order phase at binary interfaces.

The term $f(\phi)$ represents the interface driving force due to the occurrence of different bulk phases. A general formulation of $f(\phi)$ can be given as an interpolation of different free energy densities f_α of the bulk phases,

$$f(\phi) = \sum_{\alpha} f_{\alpha} h(\phi_{\alpha}) \quad (5)$$

For studying the kinematics of crystal growth, we apply the interpolation function $h(\phi_{\alpha}) = \phi_{\alpha}^3 (6\phi_{\alpha}^2 - 15\phi_{\alpha} + 10)$ as a suitable interpolaton function and a constant value for f_{α} for the bulk free energies.

The evolution equations for the phase fields can be derived from the free energy functional (1) by relating the temporal change of the order parameter, i.e. $\frac{\partial \phi_{\alpha}}{\partial t}$ to the variational derivative of the functional \mathcal{F} . Applying the Euler Lagrange formalism yields:

$$\tau \varepsilon \frac{\partial \phi_{\alpha}}{\partial t} = \varepsilon (\nabla \cdot a_{,\nabla \phi_{\alpha}}(\phi, \nabla \phi) - a_{,\phi_{\alpha}}(\phi, \nabla \phi)) - \frac{1}{\varepsilon} w_{,\phi_{\alpha}}(\phi) - f_{,\phi_{\alpha}}(\phi) - \lambda \quad (6)$$

$$\lambda = \frac{1}{N} \sum_{\alpha} \varepsilon (\nabla \cdot a_{,\nabla \phi_{\alpha}}(\phi, \nabla \phi) - a_{,\phi_{\alpha}}(\phi, \nabla \phi)) - \frac{1}{\varepsilon} w_{,\phi_{\alpha}}(\phi) - f_{,\phi_{\alpha}}(\phi) \quad (7)$$

where the comma separated subindices represent derivatives with respect to ϕ_α and gradient components $\frac{\partial \phi_\alpha}{\partial \chi_i}$. The lagrange multiplier λ guarantees the summation constraint

$\left(\sum_{\alpha=1}^N \phi_\alpha = 1 \right)$. In the evolution equation (6), τ is the kinetic coefficient which establishes a relationship between the interface growth velocity and the driving force. In the following sections, we assume negligible interface kinetic effect and choose the value of τ accordingly. This assumption ensures that the rate at which a nuclei evolves into its equilibrium shape (fast or slow growth mode), is not influenced by interface kinetics.

The phase-field evolution equation (6) is solved numerically using an explicit forward Euler scheme. The spatial derivatives of the right hand side equation are discretized using a second order accurate scheme with a combination of forward and backward finite differences. The phase-field solver is written in programming language C and only solves the evolution equation next to the locally present interfaces. The implementation of such a locally reduced order parameter optimization (LROP) facilitates a reduction in computation time from $O(N^3)$ to $O(1)$ and in memory consumption from $O(N)$ to $O(1)$ per cell in the domain, N being the number of crystals in the system. Thus, the computation is independent of the number of phases making the large scale crystal growth studies feasible even in 3D (Kim et al., 2006; Nestler et al., 2008a). Further, the simulation code is highly parallelized on the basis of message passing interface (MPI) standard including 3D domain decomposition and dynamic redistribution schemes. For the present article, the simulations are performed on multiprocessor workstations as well as on Linux high performance cluster.

3. Free growth in open cavity

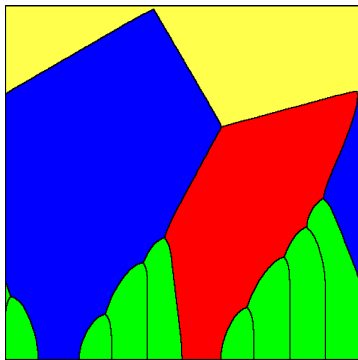
The dependence of growth rate on facet orientations for a single crystal has been reported in the past (Mügge, 1925; Mullin, 2001). However, when polycrystal growth occurs, the neighboring crystals influence the growth rate. Microstructures formed due to crystal growth in an open cavity are characterized by an increase in grain size with more favorably oriented facets out-growing the poorly oriented neighbors (Schmidegg, 1928; Thijssen et al., 1992). The orientation selection rule responsible for the growth competition in such systems is based on the difference with respect to the most preferred growth direction. In the following section, we simulate grain growth competition in 2D and 3D and deduce the orientation selection rule. Since the scope of the current study is limited to kinematics of crystal growth, the driving force is assumed to be constant.

One of the common mineral analogue that has been used to replicate free growth of crystals in laboratory experiments is Potash alum $[\text{KAl}(\text{SO}_4)_2 \cdot 12\text{H}_2\text{O}]$ (Nollet et al., 2006). The crystal structure of alum is cubic with eight $\{111\}$ facets. At room temperature it grows into an octahedral habit and also develops $\{110\}$ and $\{100\}$ facets. However, the growth rate of the $\{110\}$ and $\{100\}$ facets is much higher as compared to $\{111\}$, hence they are much smaller in size as compared to the primary facet (Bhat et al., 1992). Klapper et al. (2002) report that temperature fluctuation increases the growth rate of $\{110\}$ and $\{100\}$ facets with respect to $\{111\}$. They also state that crystal dissolution and recrystallization can lead to formation of extra facets in the early growth stages. In the present work, we limit the discussion to cubic symmetry since the kinetics of precipitation of crystals from its salt solution is yet to be incorporated in the present phase-field model. In the remaining article, we focus on simulating the $\{111\}$ facet unless otherwise stated.

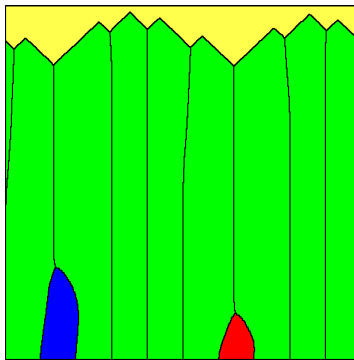
In the first set of simulations, we study the effect of non-neighboring members in the free-growth regime of cubic crystals. A 2-D simulation is carried out with 10 crystal seeds uniformly embedded at the bottom of the simulation domain and orientation designated as A, B or C degrees. In fig. 2, the second grain from left at the bottom grain boundary is assigned 'A' degrees and sixth grain as 'B' degrees. All other grains are assigned 'C' degrees. Similarly, we simulate the free-growth in 3D by embedding 36 crystal seeds uniformly at the bottom and assigning each orientation A and B once in the domain. The rest of the grains are assigned with orientation value C as shown in fig. 3. The numeric value of 'A', 'B' and 'C' are chosen to investigate the effect of non-neighboring crystals (if any) on orientation selection during free-growth of crystals.

On the basis of phase-field simulation results as shown in figs. 2a - 2f, we derive an orientation map fig. 2g of crystal orientations 'A', 'B' and 'C' to establish the following selection rules:

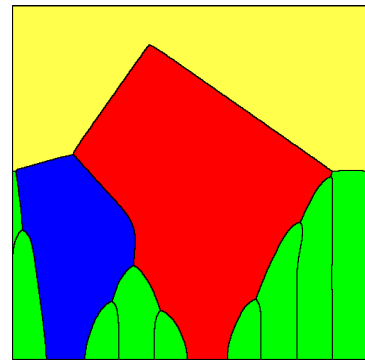
- If every crystal has a different orientation, the crystal which is most favorably oriented most preferred orientation (vertical in this case), survives and rest of the crystals are consumed.
- The consumption or survival of a crystal depends on its own orientation relative to its neighbors. The non-neighboring crystals do not effect the growth.
- Crystals retain their equilibrium shape (from Wulff construction) when in contact with liquid at all times.
- Crystals having the same growth orientation with respect to most preferred orientation (vertical in this case) form perpendicular grain boundaries and co-exist in the final microstructure, if the other neighboring crystals are not more favorably ori-



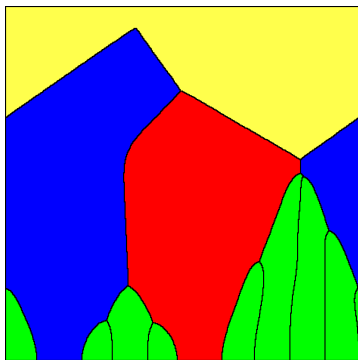
(a)



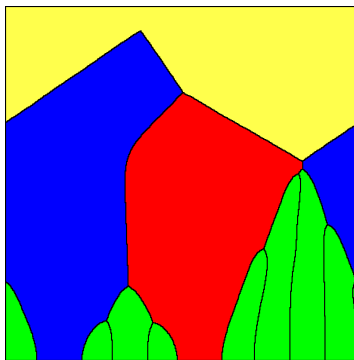
(b)



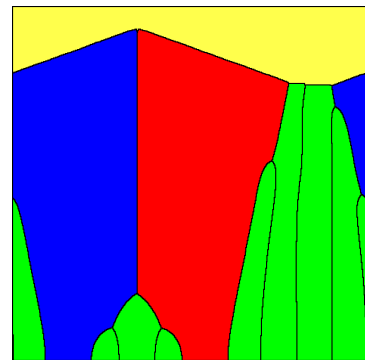
(c)



(d)



(e)



(f)

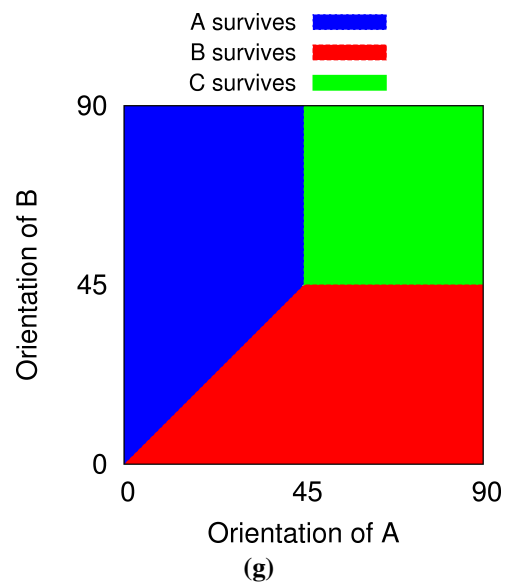


Figure 2: Anisotropic growth competition of crystals with orientation A (blue), B (red) and C (green). (a) $A = 15^\circ$, $B = 30^\circ$ and $C = 45^\circ$ (b) $A = 15^\circ$, $B = 30^\circ$ and $C = 0^\circ$ (c) $A = 30^\circ$, $B = -5^\circ$ and $C = 45^\circ$ (d) $A = 10^\circ$, $B = -15^\circ$ and $C = 45^\circ$ (e) $A = 11^\circ$, $B = -15^\circ$ and $C = 45^\circ$ (f) $A = 25^\circ$, $B = -25^\circ$ and $C = 45^\circ$ (g) Orientation map for $C = 45^\circ$ derived from phase-field simulation results.

ented. This is also observed in 3D case when two crystals have a similar orientation with respect to vertical line but lie in different planes.

Next, we perform a 3D simulation of alum crystal growth such that crystals also develop $\{110\}$, and $\{100\}$ facets in addition to $\{111\}$ as shown in fig. 4. Hemispherical crystal seeds are uniformly embedded at the bottom of the domain as shown in fig. 4a, and every crystal is assigned a random orientation with respect to the normal direction of the growth plane. The growth results in consumption of poorly oriented crystals (greenish and bluish in color) and in survival of favorably oriented (reddish) as shown in fig. 4c.

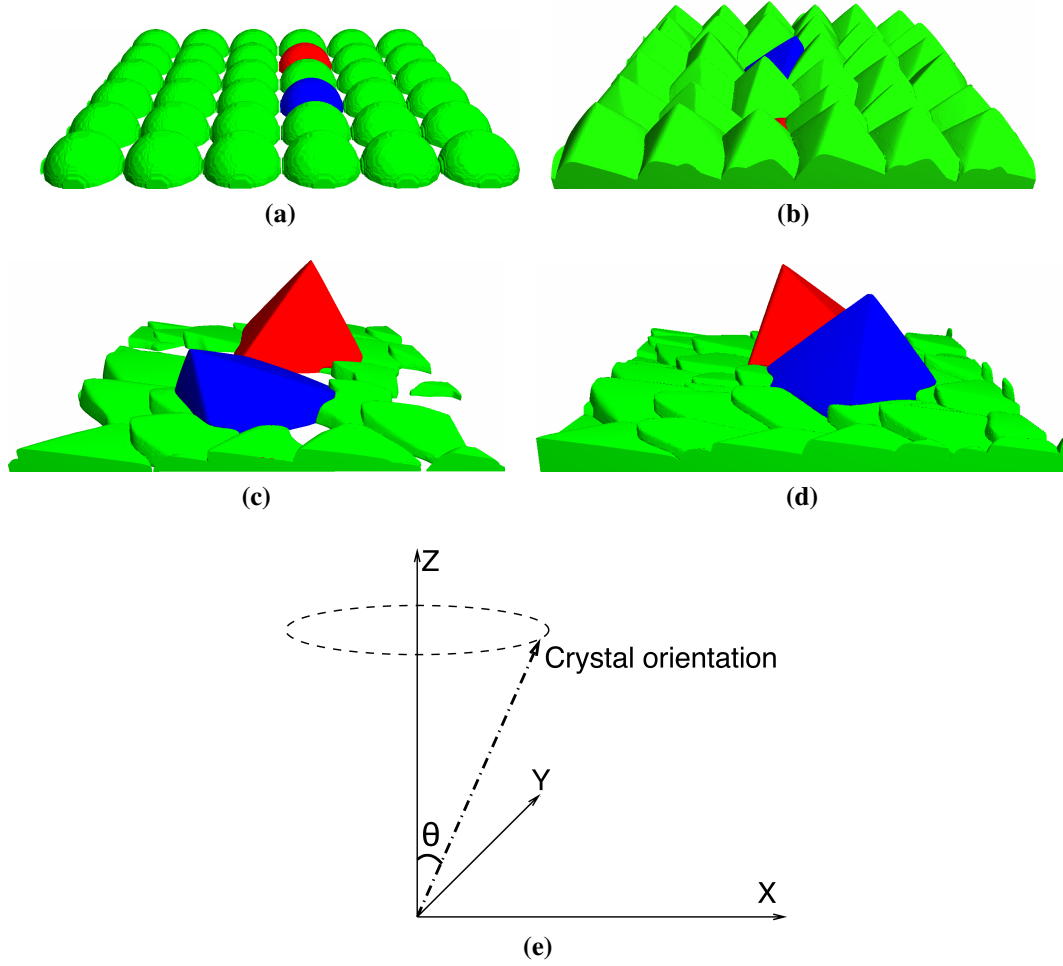


Figure 3: 3D phase-field simulation of cubic crystal growth: (a) Initial condition with hemispherical nuclei uniformly embedded at the bottom of the domain and with assigned orientations of A (blue), B (red) and C (green) degrees. Growth competition leads to orientation selections according to the orientations (b) $A = 15^\circ$, $B = 30^\circ$ and $C = 0^\circ$ (c) $A = -30^\circ$, $B = 5^\circ$ and $C = 45^\circ$ (d) $A = 15^\circ$, $B = -10^\circ$ and $C = 45^\circ$ (e) Schematic drawing to define the orientation with respect to x, y and z axes.

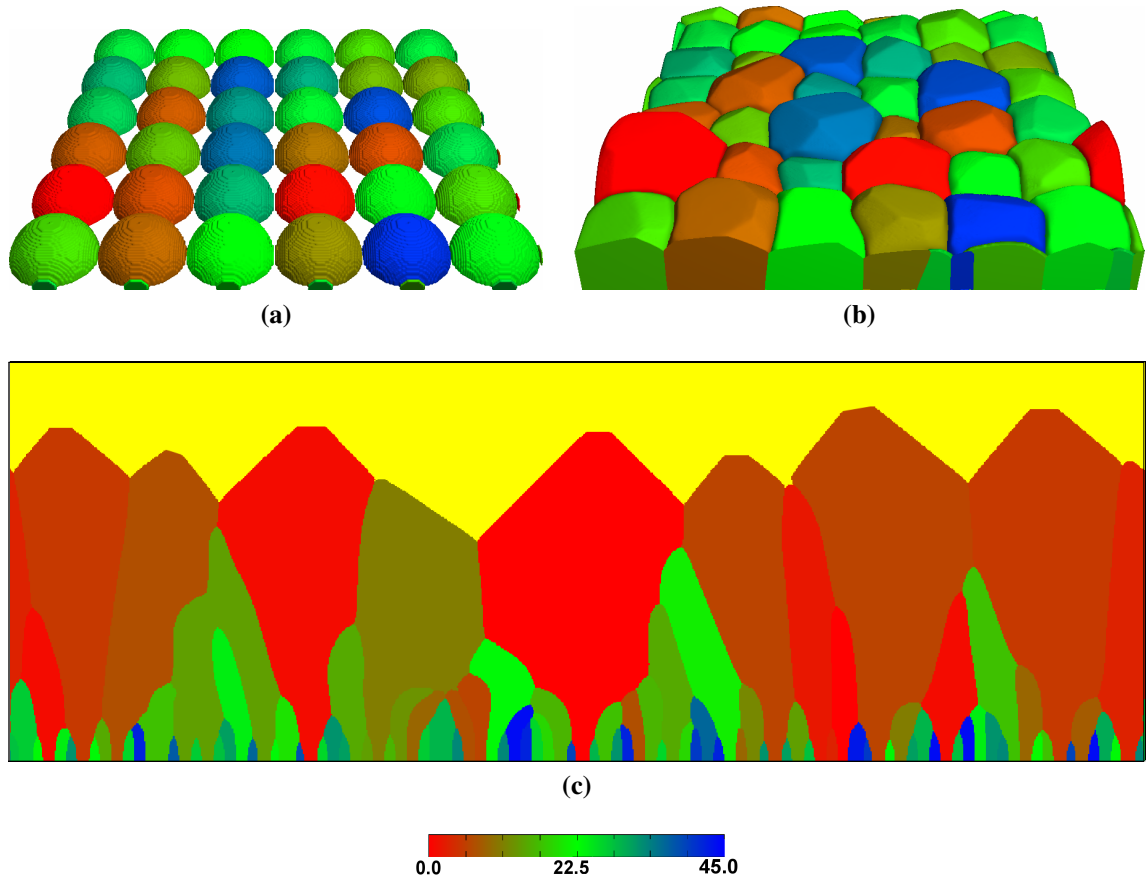


Figure 4: Free growth of alum crystals with random orientations. (a) Bottom layer of the 3D phase-field simulation domain showing the spherical crystal nuclei and their assigned orientations in different colors. (b) intermediate stage of alum crystals growing in liquid. The facets $\{111\}$, $\{110\}$ and $\{100\}$ can be distinctly identified, (c) 2D simulation showing the final stage of growth competition. Favorably oriented crystals (reddish) outgrow their neighbors.

4. Crack-seal growth

In the following section, we use the phase-field method described in section 2, to study the effect of various crack parameters namely roughness, opening velocity and trajectory on the crack-seal microstructure. Further, we also examine if the number of competing crystal nuclei causes a variation in the final microstructure.

Numerical simulations are carried out with periodic asperities on the crack wall and uniformly distributed crystal nuclei placed at the top of the domain. The crystals grow downwards in the direction of crack opening. All the crystals are assumed to possess a cubic anisotropy and assigned an orientation randomly in the range of -45° to 45° with respect to vertical direction.

4.1. Effect of crack wall roughness

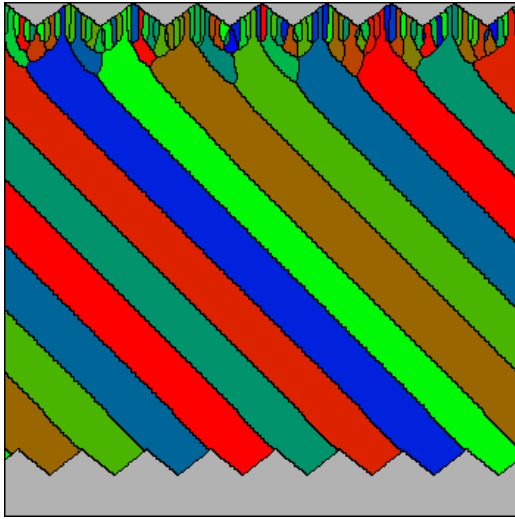
The crack surface is assumed to be periodic and the degree of roughness is controlled by the vertical angle β which is varied between 90° and 180° while keeping the wavelength constant, as shown in fig. 5f. An angle of $\beta = 180^\circ$ corresponds to a smooth surface. The crack is opened periodically at an angle θ_{open} with respect to the vertical direction. In order to study the influence of crack roughness, we fix the value of θ_{open} to be 45° . The velocity of crack opening is selected in such a way that complete sealing of crack occurs before every crack opening event.

At a higher crack roughness ($\beta = 90^\circ$), it is observed in fig. 5a that the crystals track the crack opening trajectory. This is also characterized by the crack crest attracting the grain boundaries and forcing the crystals to grow in a fibrous morphology. As the roughness angle β is successively increased in figs. 5b - 5d, the tracking behavior decreases and crystals develop curved/oscillating grain boundaries. The period of oscillation reduces with decreasing roughness.

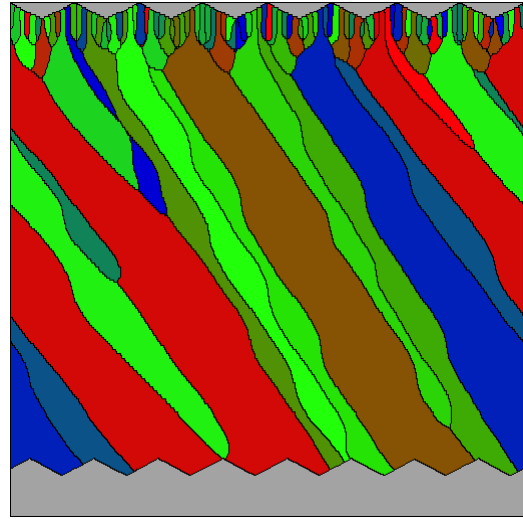
To quantify the grain boundary tracking behavior, we plot the contour of the crystal grain boundaries (corresponding to $\phi = 0.5$) and fit straight lines to the left and right crystal boundaries as illustrated in fig. 5e. The overall tracking inclination θ_{track} is defined as the mean value of the slopes of the two lines and is used to elaborate the tracking efficiency (TA) as

$$TA = \frac{\theta_{track}}{\theta_{open}} \quad (8)$$

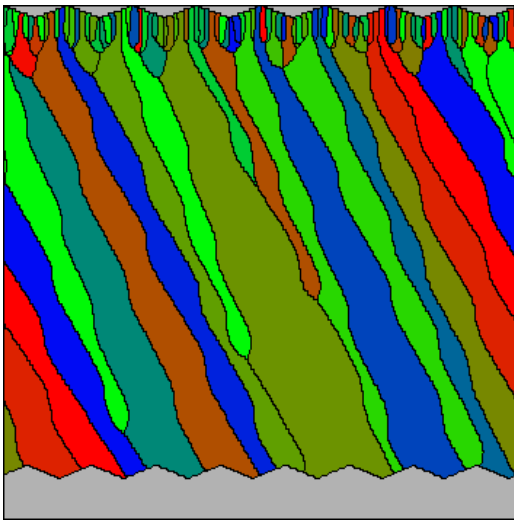
The tracking efficiency (TA) is plotted as a function of roughness angle β in fig. 5f. The resulting trend indicates that the tracking efficiency decreases for lower crack-surface roughness, beyond a certain β value.



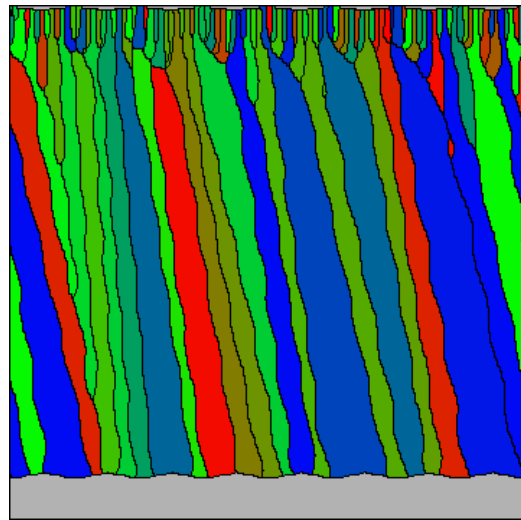
(a)



(b)



(c)



(d)

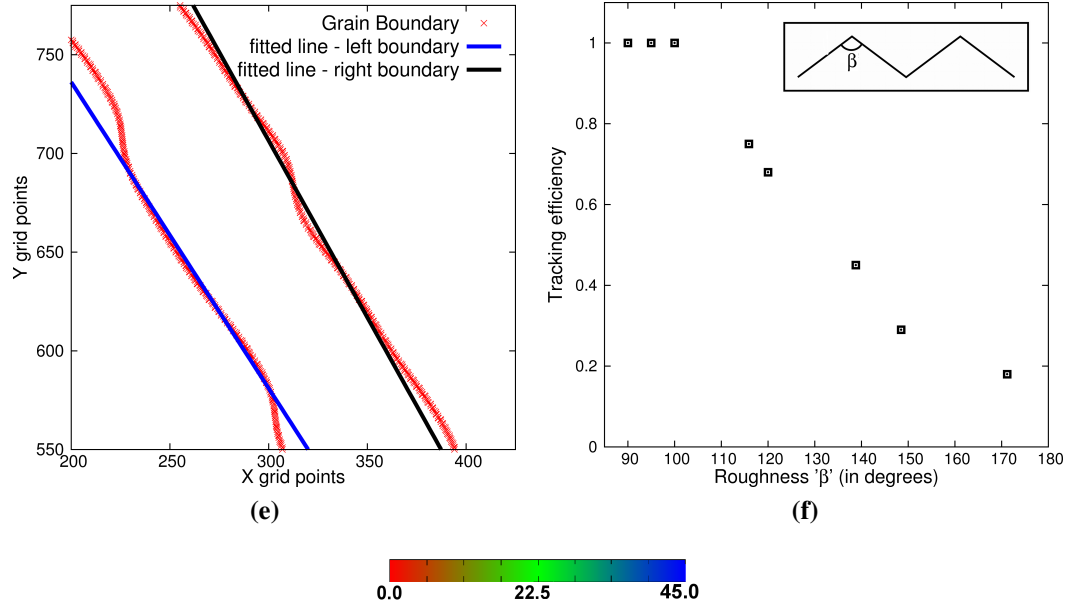


Figure 5: Effect of crack-wall roughness on the grain boundary tracking behavior. The direction of the crack opening is $\theta_{open} = 45^\circ$ to the vertical line. The simulated grain structures refer to wall roughness of (a) 100° , (b) 120° , (c) 139° and (d) 171° (e) straight lines are fitted along the grain boundaries corresponding to $\phi = 0.5$ (f) plot of tracking efficiency as a function of crack roughness. The colors refer to different crystal orientation with respect to the vertical direction (see colormap).

4.2. Effect of crack opening rate

To study the effect of crack opening velocity on vein growth, a simulation setup similar to section 4.1 is considered with 10 crystal nuclei. The roughness angle $\beta = 100^\circ$ is selected to ensure a high level of tracking efficiency, if complete sealing occurs before every opening event. The crack opening angle is kept constant ($\theta_{open} = 45^\circ$) and rate of opening is varied as shown in fig. 6. It is observed in fig. 6a that at higher crack opening rate (as compared to crystal growth rate), crystals lose contact with the crack surface. This leads to the formation of elongate-blocky growth morphology, since crystals now grow more or less anisotropically and follow the orientation rule as observed for free-growth in fig. 2g. At lower crack opening rate as in figs. 6b and 6c, crystals grow isotropically in fibrous morphology, since the facet formation is suppressed. Further, within the complete crack-seal regime, at a higher opening velocity, the crystal boundaries have a tendency to curve in contrast to the case when opening velocity is smaller. The simulation results for the influence of crack opening velocity on crystal growth morphology are presented in fig. 6. A definitive change in the crystal growth morphology is observed if crack opening rate is varied.

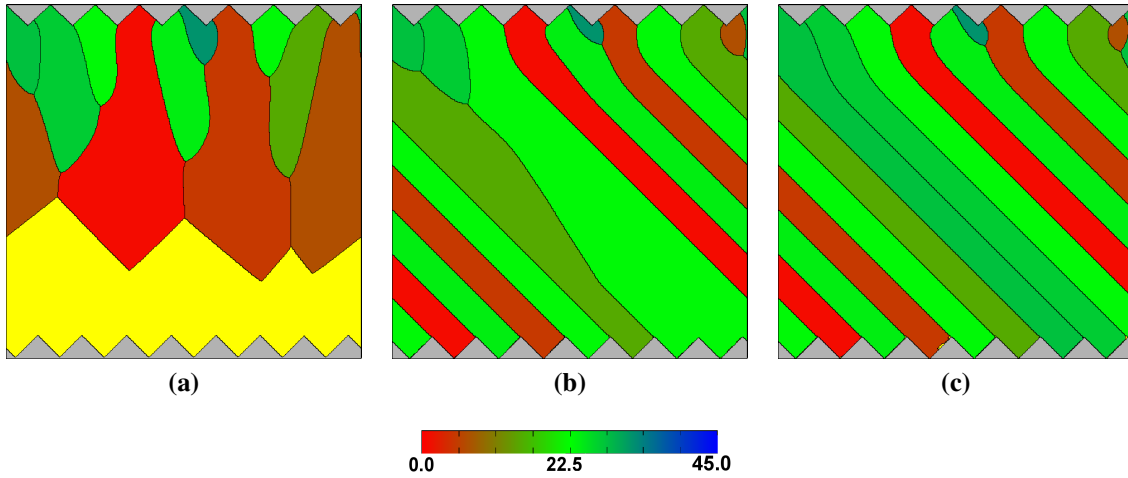


Figure 6: Effect of crack-wall opening velocity on crystal growth morphology and final microstructure. The growth is elongate-blocky at higher crack opening rate in contrast to fibrous when the crack opening rate is slower. Further, within the complete crack seal regime, a morphological transition from curved to straight boundaries is observed. The direction of the crack opening is 45° with respect to vertical. The crack opens every (a) 200, (b) 500 and (c) 700 timesteps. The colors refer to different crystal orientation with respect to vertical (see colormap).

4.3. *Effect of crack opening trajectory*

In the next series of simulations, 100 crystal nuclei with different orientation are uniformly embedded at the top of the domain and the crack opening angle θ_{open} is varied. The crack roughness angle β is selected to be 100° and a complete sealing is ensured at every opening event. The phase-field simulation results show that crystals track the crack opening trajectory, irrespective of θ_{open} . Thus, the grain boundary tracking efficiency is not affected by the crack opening angle. The results of the simulation are summarized in fig. 7. On further increasing the magnitude of the crack opening increment in fig. 8 while ensuring complete sealing before every opening event, we observe that the tracking behavior is lost and crystals grow in a random morphology (fig. 8a). However, when the crack opening increment is reduced ten-folds, while keeping θ_{open} unchanged, crystals re-establish a tracking of the crack opening trajectory as shown in fig. 8b.

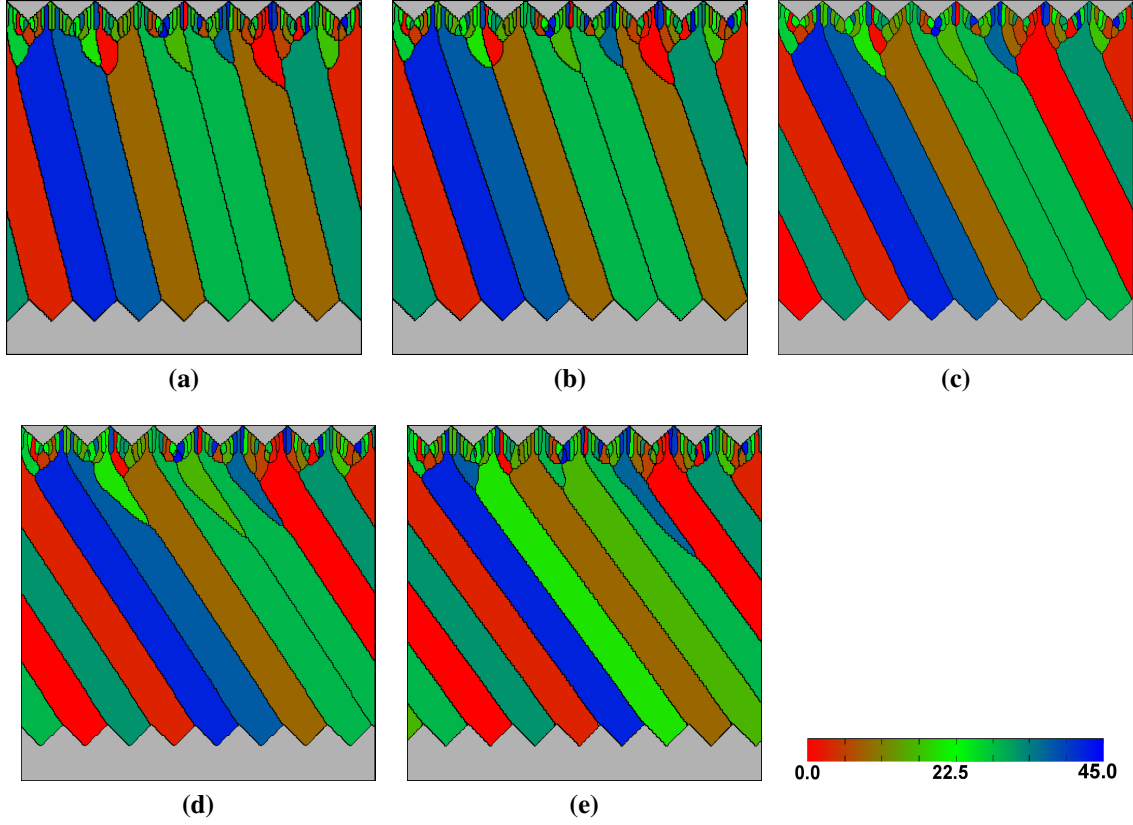


Figure 7: Effect of crack opening trajectory on crack-seal microstructure. The angles of opening θ_{open} are (a) 14.0° , (b) 18.4° , (c) 26.5° , (d) 33.6° and (e) 36.8° with respect to vertical in anti-clockwise direction. The crystals track the crack opening irrespective of the trajectory, if opening increments are small and crack surface is sufficiently rough. The colors refer to different crystal orientation with respect to the vertical direction (see colormap).

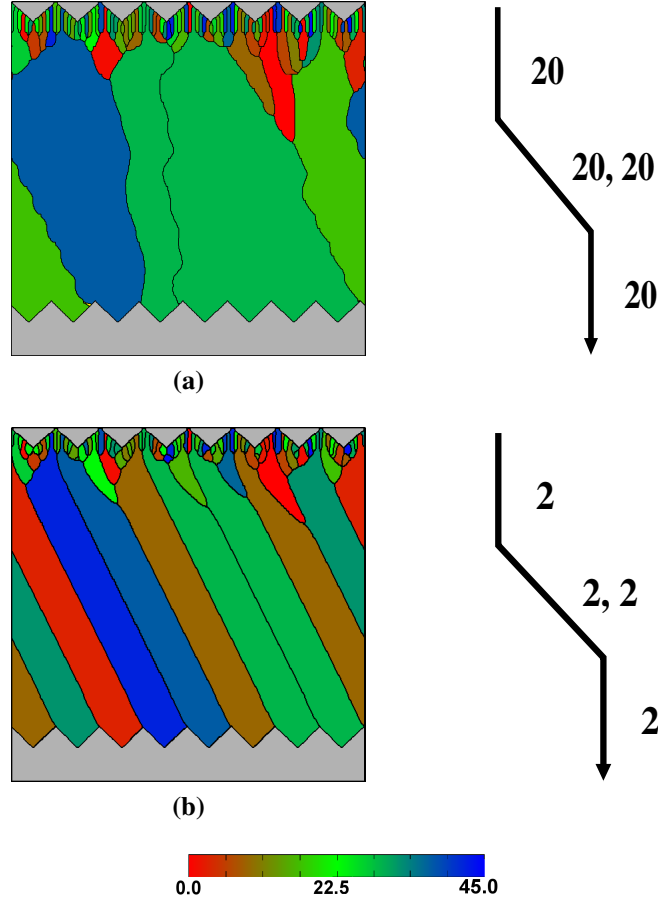


Figure 8: Effect of crack opening increment on the crack-seal microstructure. The same number of crystal nuclei, crystal anisotropy and wall morphology are used as in fig. 7. (a) Loss of tracking behavior for linear and oblique opening in large increments (20 grid-points lateral offset). (b) Grain boundary tracking for linear and oblique opening in smaller increments (2 grid-points lateral offset). Crystals track the opening trajectory only when opening increments are sufficiently small. The colors refer to different crystal orientation with respect to the vertical direction (see colormap).

4.4. Effect of number of crystal nuclei

The number of nuclei is varied to study its influence on the vein growth morphology. The crack is assumed to be sufficiently rough for 100% tracking of crystal boundaries and complete sealing is ensured. The phase-field simulations show that varying the initial number of nuclei does not influence the tracking behavior. It is noteworthy that the number of surviving crystals remains constant and is numerically equal to the number of peaks in the crack surface which faces the crystal growth front. The crystal boundaries stabilize at the crack peaks which suggest that these attract the grain boundaries. Further, we do not observe any change in growth morphology once the number of crystals surviving equals the crack peaks, irrespective of the initial number of nuclei as shown in fig. 9.

Finally, 3D phase-field simulations of crack-sealing are carried out by embedding 100 crystal nuclei on computationally generated rough crack surface in figs. 10a and 10b. The roughness of the 3D crack surface is controlled by varying the range of amplitude of peaks. The crack is opened slowly to ensure ensuring complete sealing before every opening event. The 3D simulation results are displayed in fig. 10 which shows a layer-by-layer plot of the simulation domain. The simulation results reveal that a crack surface with higher roughness forces the crystals to track the opening trajectory. As the surface roughness is reduced, the resulting grain boundaries partially form curved/oscillatory morphologies (fig. 10d). It can be observed, that crystals grow in a mixed regime when the wall roughness is not sufficiently high.

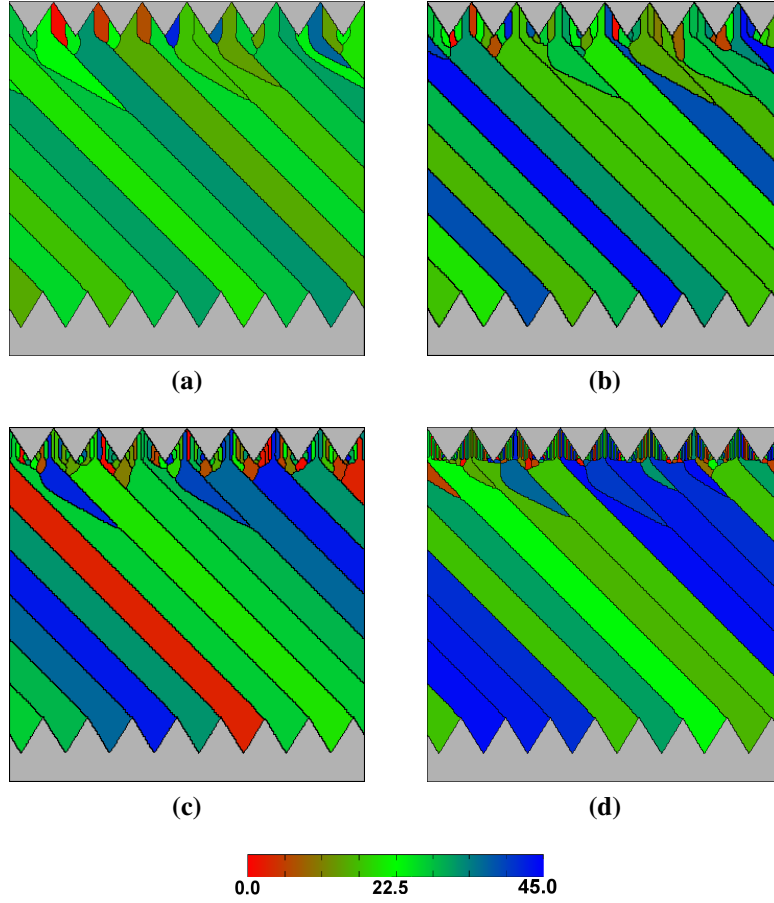
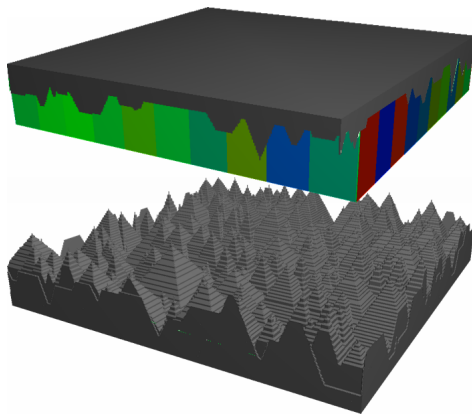
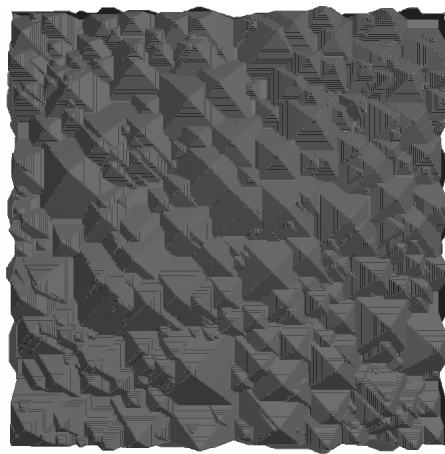


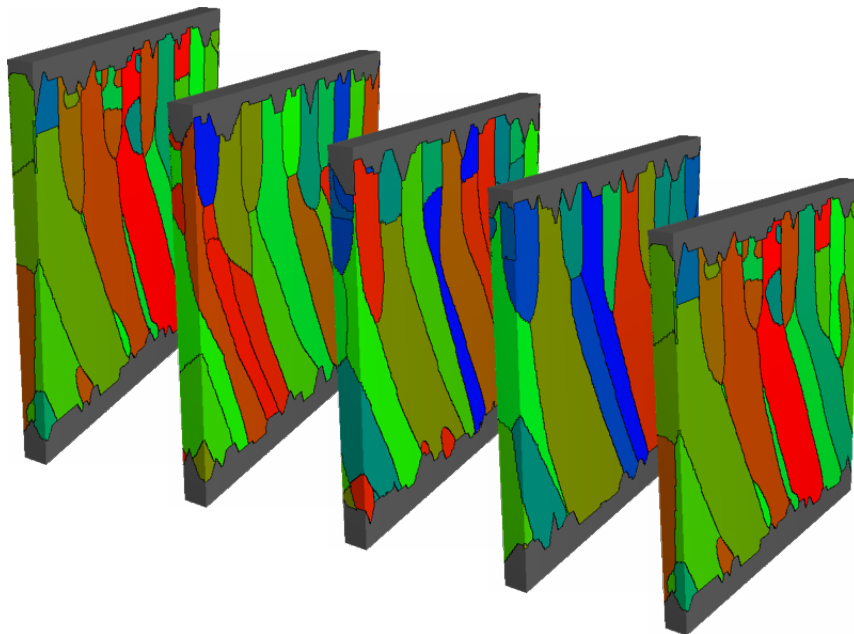
Figure 9: Effect of initial number of nuclei on crystal growth morphology and final microstructure. The crack opening increments are small in the direction 45° with respect to vertical. The crack surface facing the crystal growth front has 8 peaks. The number of crystal nuclei are varied as in (a) 25, (b) 50, (c) 100 and (d) 250 to observe the effect on final microstructure. The number of crystals that end up tracking the crack openings is equal to the number of peaks on the advancing crack. Colors refer to different crystal orientation with respect to vertical (see colormap).



(a)



(b)



(c)

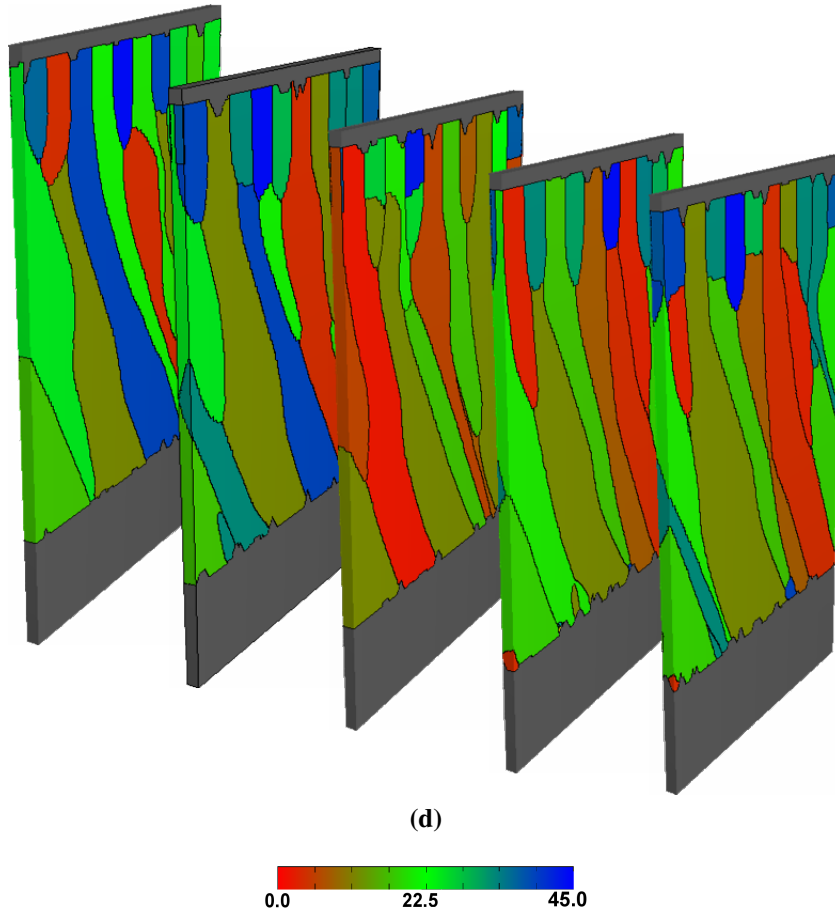


Figure 10: Crystals are embedded on an algorithmically irregular surface for simulating crack-sealing process in 3D. The crack surface roughness is defined by the amplitude of peaks. To reduce the surface roughness, the amplitude of every peak is reduced by a numeric factor. (a) The initial simulation domain setting. (b) Top view of the crack surface. (c) 3D layer plot of the phase-field simulation of crack-sealing process showing (c) grain boundary tracking along with occasional occurrence of curved boundaries for the roughness factor 6 and for a crack opening velocity of 2 grid points lateral offset, in (d), the number of curved/inflected grain boundaries increases for the roughness factor 10 and for a crack opening velocity of 4 grid points lateral offset. The crack opening trajectory is similar as observed in 3D in fig. 8b. Colors refer to different crystal orientation with respect to vertical direction (see colormap).

5. Discussion of results

In the present article, the multi-phase-field model for grain-growth has been extended to study the crystal growth in veins in two different growth conditions namely, free-growth in fluid and crack-sealing. The previous algorithm for modeling vein growth (Bons, 2001) neglects the role of surface energy anisotropy, which is responsible for crystal facet formation and growth competition. This leads to deviations of simulation results when compared with natural microstructures. The phase-field model presented in this article explains the role of surface energy anisotropy and additionally takes into account, the interface thermodynamics and force balances at multi-grain junctions (crystal triple/quadruple points in current context). Thus, the selection dynamics of faceted crystal growth observed in present simulations compare well with the experimental findings (Hilgers and Urai, 2002a).

It is observed that the consumption or the survival of a crystal depends on its own orientation relative to neighbors, when allowed to grow freely. The non-neighboring crystals do not effect the growth of the crystal in consideration directly. Additionally, the inter-facet angle defined by the equilibrium shapes are always preserved for the crystals growing freely in liquid figs. 1c and 1d. Moreover, we do not observe any exceptions in the deduced crystal growth selection rule contrary to the findings of Nollet et al. (2005) for cubic crystal symmetry. The phase-field simulation results in figs. 2d and 2e corroborate the findings of Bons and Bons (2003) by the observation that the interface boundary between crystal 'A' and 'B' is found to be inflected. Apparently, if sufficient time is available for the development of facets, the favorably oriented crystals always out-grow the poorly oriented neighbors. We are aware of the fact that crystal growth results from an interplay of surface energy anisotropy and growth kinetics. Typically, a crystal nucleates in its equilibrium (Wulff) shape and grows asymptotically towards its "kinetic Wulff shape" if long-range transport of energy and/or mass is assumed to be extremely fast (Sekerka, 2005). Additionally, we do not rule out the possibility of different contact angles at liquid–solid triple junctions as a result of different force balances corresponding to kinetic or surface energy anisotropy. Therefore, the values of the kinetic coefficient τ and of interfacial energies need to be chosen appropriately to simulate correct selection dynamics.

The presence of a barrier for example, a rigid and rough crack surface, obstructs the freely growing crystals, forcing them to grow into a morphology unrelated to the equilibrium crystal shape. It is found that the crack parameters such as the roughness, opening velocity and trajectory determine the final crack-seal microstructure. The phase-field simulation results of crack-sealing process suggest that if the wall rock is sufficiently rough and opening velocity is small, the crystals grow isotropically, in a fibrous morphology

and track the crack-opening trajectory. In this case, anisotropy in surface energy does not effect the growth morphology since facet formation is suppressed due to the additional boundary condition, which corroborates the previous simulation and experimental studies on crack-sealing process (Hilgers et al., 2001; Nolle et al., 2005; Urai et al., 1991). Moreover, higher number of peaks/kinks or the degree of roughness of the facing wall rock, also increases the fineness of fibrous microstructure. This is inferred from fig. 9 which shows that if roughness is sufficiently high, the number of fibers formed is numerically consistent with the peaks/kinks on the facing crack surface. At a lower crack surface roughness, the grain boundary tracking efficiency decreases and the crystal boundaries have a curved/oscillating morphology as presented in figs. 5b, 5c and 5d. The anisotropy of the surface energy provides an explanation for the curvature observed in grain boundaries in this case, as the crack opening events occur along an oblique 45° line with respect to vertical direction. It is noteworthy, that grain boundaries alone do not provide much information about the crack-opening trajectory in such cases. The simulation results also reveal that straight grain boundaries are formed when surface energy of the growing crystals is assumed to be isotropic. Further, within the complete crack-seal regime, when the opening increment is on a relatively higher side, curved grain boundaries are formed. The 3D phase-field study of crack-sealing process accentuate these findings; if the wall rock roughness is low and crack opening velocity is increased while still ensuring complete sealing before every opening event, the crystals growth occurs in a mixed regime, characterized by a decrease in tracking behavior with a propensity to form curved grain boundaries. A systematic study to establish the correlation of crack roughness and opening rate with the extent/amplitude of grain boundary curvature/oscillation and influence of hydrodynamic convection, is a part of on-going effort.

6. Conclusion and outlook

In the present article, the parameters controlling the vein microstructure are studied using the phase-field method. The role of surface energy anisotropy during free growth of crystals and its influence on the grain orientation selection is addressed. The 3D phase-field simulation of free crystal growth process provides further insight on how poorly oriented crystals are consumed by more favorably oriented ones and previous ambiguities reported in literature (Nolle et al., 2005) are ruled out. Further, the influence of crack parameters on the final microstructure is discussed in detail. One of the intriguing finding of the current work is the role of surface energy anisotropy in the formation of crack-seal microstructures. Of particular importance, is the appearance of curved/oscillating crystal boundaries which draws similarities with the natural vein microstructures. It is noteworthy, that such effects are not reported in previous simulations as the anisotropy in surface

energy of crystals is neglected. The current phase-field study of crack-sealing process (in 2D and 3D) indicate that anisotropy in surface energy of the growing crystals cause the grain boundaries to curve/oscillate, if wall rock is not sufficiently rough and crack opening rate is increased gradually while still ensuring complete crack-sealing before every opening event. The fineness of the fibrous microstructure is directly related to the number of peaks/kinks on the facing wall surface. Further, the transition from fibrous to elongate-blocky morphology in vein microstructure caused by varying the crack opening rate is demonstrated in the simulation results.

The present work also establishes the phase-field method as comprehensive and stand-out approach to simulate the geological processes occurring during vein formation. The simulation results also demonstrate the general capability of multi-phase-field method in dealing with anisotropic 3D vein-growth problem. Since the underlying model equations are based on continuum mechanical and thermodynamical concepts, several extensions of the present vein-growth model are possible. This includes the studies related to diffusion driven grain evolution and hydrodynamic convection. Including such effects in the present phase-field model is imperative for the complete understanding of the vein growth problem. Once implemented, the model can be further utilized to study the precise effect of hydrodynamic convection on the morphology of the vein front and crystal boundaries. Further, this also helps in debating the question posed by Barker et al. (2006) whether vein formation involves advective fluid flow, or occurs by local diffusion of material from the surrounding wall rock. Though, this requires significant computational resources, the efficient parallelization of the phase-field solver (Nestler et al., 2008a) (utilized for phase-field simulations presented in this article) makes it feasible.

Acknowledgements

Abhik Choudhury (from Ecole Polytechnique (CNRS), Paris) and Frank Wendler (from IAM-ZBS, KIT) are thanked for many insightful discussions. The support extended by Tomas Longo (IAM-ZBS, KIT) for visualization of 3D data is gratefully acknowledged. KA and BN acknowledge the financial support by Graduate school 1483 of German Research Foundation and by the project CCMSE of the European Union (EFRE) together with the state Baden-Wuerttemberg. KA also thanks former co-workers Denis Pilipenko and Michael Fleck (MPS, University of Bayreuth) for preliminary discussions concerning the model and Center for Computing and Communication at RWTH Aachen University (HPC Cluster) for computational resources.

References

- Barker, S.L., Cox, S.F., Eggins, S.M., Gagan, M.K., 2006. Microchemical evidence for episodic growth of antitaxial veins during fracture-controlled fluid flow. *Earth Planet. Sc. Lett.* 250, 331 – 344.
- Bhat, H.L., Ristić, R.I., Sherwood, J.N., Shripathi, T., 1992. Dislocation characterization in crystals of potash alum grown by seeded solution growth under conditions of low supersaturation. *J. Cryst. Growth* 121, 709 – 716.
- Bons, A.J., Bons, P.D., 2003. The development of oblique preferred orientations in zeolite films and membranes. *Micropor. Mesopor. Mat.* 62, 9 – 16.
- Bons, P.D., 2001. Development of crystal morphology during unitaxial growth in a progressively widening vein: I. the numerical model. *J. Struct. Geol.* 23, 865 – 872.
- Bons, P.D., Jessell, M.W., 1997. Experimental simulation of the formation of fibrous veins by localised dissolution-precipitation creep. *Mineralogical Mag.* 61, 53–63.
- Cox, S.F., Etheridge, M.A., 1983. Crack-seal fibre growth mechanisms and their significance in the development of oriented layer silicate microstructures. *Tectonophysics* 92, 147 – 170.
- Cox, S.F., Etheridge, M.A., Wall, V.J., 1987. The role of fluids in syntectonic mass transport, and the localization of metamorphic vein-type ore deposits. *Ore Geol. Rev.* 2, 65–86.
- Durney, D.W., 1976. Pressure-solution and crystallization deformation. *Philos. T. R. Soc. S-A* 283, 229–240.
- Durney, D.W., Ramsay, J.G., 1973. *Gravity and Tectonics*. New York: Wiley. chapter Incremental Strains Measured by Syntectonic Crystal Growths. pp. 67–96.
- Fisher, D.M., Brantley, S.L., 1992. Models of quartz overgrowth and vein formation: deformation and episodic fluid flow in an ancient subduction zone. *J. Geophys. Res.* 97, 20,043–20,061.
- Hilgers, C., Koehn, D., Bons, P.D., Urai, J.L., 2001. Development of crystal morphology during unitaxial growth in a progressively widening vein: II. numerical simulations of the evolution of antitaxial fibrous veins. *J. Struct. Geol.* 23, 873 – 885.
- Hilgers, C., Urai, J.L., 2002a. Experimental study of syntaxial vein growth during lateral fluid flow in transmitted light: first results. *J. Struct. Geol.* 24, 1029 – 1043.

- Hilgers, C., Urai, J.L., 2002b. Microstructural observations on natural syntectonic fibrous veins: implications for the growth process. *Tectonophysics* 352, 257 – 274.
- Jamtveit, B., Yardley, B.W.D., 1997. *Fluid Flow and Transport in Rocks: Mechanisms and Effects*. Chapman & Hall.
- Kim, S.G., Kim, D.I., Kim, W.T., Park, Y.B., 2006. Computer simulations of two-dimensional and three-dimensional ideal grain growth. *Phys. Rev. E* 74, 061605.
- Klapper, H., Becker, R.A., Schmiemann, D., Faber, A., 2002. Growth-sector boundaries and growth-rate dispersion in potassium alum crystals. *Cryst. Res. Technol.* 37, 747–757.
- Knipe, R.J., McCaig, A.M., 1994. Microstructural and microchemical consequences of fluid flow in deforming rocks.
- Koehn, D., Hilgers, C., Bons, P.D., Passchier, C.W., 2000. Numerical simulation of fibre growth in antitaxial strain fringes. *J. Struct. Geol.* 22, 1311 – 1324.
- McCaig, A.M., 1988. Deep fluid circulation in fault zones. *Geology* 16, 867–870.
- Mügge, Ö., 1925. Über gehemmtes kristallwachstum. *Z. Kristallogr.* 62, 415–442.
- Mügge, Ö., 1928. Ueber die entstehung faseriger minerale und ihrer aggregationsformen. *Neues. Jahrb. Miner. Geol. P. A* 58, 1928.
- Mullin, J.W., 2001. Fourth edition ed.. Butterworth-Heinemann. chapter Crystal Growth.
- Nestler, B., Garcke, H., Stinner, B., 2005. Multicomponent alloy solidification: Phase-field modeling and simulations. *Phys. Rev. E* 71, 041609.
- Nestler, B., Reichardt, M., Selzer, M., 2008a. Massive multi-phase-field simulations: methods to compute large grain system, in: Hirsch, J., Skrotzki, B., Gottstein, G. (Eds.), *Proceedings of the 11th International Conference on Aluminium Alloys*, Aachen, Germany. pp. 1251–1255.
- Nestler, B., Wendler, F., Selzer, M., Stinner, B., Garcke, H., 2008b. Phase-field model for multiphase systems with preserved volume fractions. *Phys. Rev. E* 78, 011604.
- Nollet, S., Hilgers, C., Urai, J.L., 2006. Experimental study of polycrystal growth from an advecting supersaturated fluid in a model fracture. *Geofluids* 6, 185–200.

- Nollet, S., Urai, J.L., Bons, P.D., Hilgers, C., 2005. Numerical simulations of polycrystal growth in veins. *J. Struct. Geol.* 27, 217 – 230.
- Ramsay, J.G., 1980. The crack-seal mechanism of rock deformation. *Nature* 284, 135–139.
- Ramsay, J.G., Huber, M.I., 1983. *The Techniques of Modern Structural Geology: Strain analysis. The Techniques of Modern Structural Geology*, Academic Press.
- Schmidegg, O., 1928. Über geregeltes wachstumsgefüge. *Jb. Geol. B.-A.* 78, 1–51.
- Sekerka, R.F., 2005. Equilibrium and growth shapes of crystals: how do they differ and why should we care? *Cryst. Res. Technol.* 40, 291–306.
- Stinner, B., Nestler, B., Garcke, H., 2004. A diffuse interface model for alloys with multiple components and phases. *SIAM J Appl. Math.* 64, 775–799.
- Taber, S., 1918. The origin of veinlets in the silurian and devonian strata of central new york. *J. Geol.* 26, pp. 56–73.
- Thijssen, J.M., Knops, H.J.F., Dammers, A.J., 1992. Dynamic scaling in polycrystalline growth. *Phys. Rev. B* 45, 8650–8656.
- Urai, J.L., Williams, P.F., van Roermund, H.L.M., 1991. Kinematics of crystal growth in syntectonic fibrous veins. *J. Struct. Geol.* 13, 823 – 836.
- Williams, P.F., Urai, J.L., 1989. Curved vein fibres: an alternative explanation. *Tectonophysics* 158, 311 – 333.
- Yardley, B.W.D., Jamtveit, B., 1997. *Fluid flow and transport in rocks : mechanisms and effects*, Chapman & Hall, London.
- Zhang, J., Adams, J.B., 2002. Facet: a novel model of simulation and visualization of polycrystalline thin film growth. *Model. Simul. Mater. Sc.* 10, 381.